Journal of Nonlinear Analysis and Optimization
Volume 15(2) (2024)
http://ph03.tci-thaijo.org
ISSN : 1906-9685

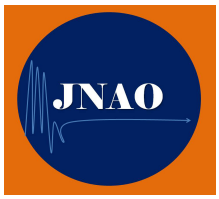

J. Nonlinear Anal. Optim.

FOMITE FACTORS AND SILENT SPREAD: A VSEIQCR STUDY OF VIRAL DISEASES

MOHIT SONI*[1], RAJESH KUMAR SHARMA[2] AND SHIVRAM SHARMA[3]

[1] Government Holkar (Model , Autonomous) Science College, Indore, Madhya Pradesh, India
[2] Government Post Graduate College, Shujalpur, Madhya Pradesh, India
[3] PMCOE, Govt. P. G. College, Guna, Madhya Pradesh, India , Krantiveer Tatya Tope University Guna, Madhya Pradesh, India

ABSTRACT. This study investigates the impact of both detected and undetected viral cases, alongside environmental pathogens, on infection transmission dynamics. A VSEIQCR model is formulated and refined to analyze the study and to assess the basic reproduction number using the next-generation matrix method. The findings reveal a rapid escalation in viral cases, correlating with the rise in undetected cases. The study suggests that identifying and isolating individuals exposed to or infected by the virus, whether detected or undetected, is deemed imperative for curtailing disease transmission. Additionally, The study emphasizes the role of fomites in infection spread. It stands out for its innovative approach, examining the interconnections among vaccination, quarantine, and contamination strategies within a cohesive research framework, thereby setting a precedent in the field.

Key words: Epidemic model, Basic reproduction number, Next-generation method, Environment pathogens (Fomites).

AMS Subject Classification: : 93C10, 93C35

1. Introduction

Some viral diseases can spread through the presence of saliva in the environment [5]. On January 30, 2020, in response to the recommendations of the Emergency Committee, the Director-General of the World Health Organization (WHO) declared the outbreak of COVID-19 a Public Health Emergency of International Concern (PHEIC) [20]. Due to its worldwide spread, the WHO [5] declared it a pandemic on March 11, 2020. COVID-19, caused by Severe Acute Respiratory Syndrome Coronavirus-2 (SARS-CoV-2), first emerged in China in December 2019 [1], [11],

* *Corresponding author.*
Email address : sonimohit895@gmail.com (M. Soni), Raj_rma@yahoo.co.in (R. K. Sharma), dr.shivramsharma@mp.gov.in (S. Sharma).
Article history : Received 26/02/2024 Accepted 12/11/2024.

[20]. Contact tracing and quarantine are key strategies adopted by India to control transmission and mortality [5]. However, when interviewing individuals infected with COVID-19 for contact tracing, some contacts may be omitted due to recall bias. These missed cases, which remain asymptomatic throughout the incubation period (2-14 days), increase the risk of involuntary transmission to the community [20]. As a result, it is essential to investigate their role in the spread of the disease. Many research articles have attempted to understand the dynamics of transmitting this disease with the help of mathematical modeling. Kermack and McKendrick [6], [7], [8] framed the initial SIR (Susceptible, infected, recovered) compartmental model to study the dynamics of a disease. Mandal et al. [9] have designed an SEIR (Susceptible, Exposed, Infected, Recovered) model to prevent or delay local outbreaks by imposing travel restrictions in India from countries affected by COVID-19. Since these studies focused on the risk of disease through direct transmission between humans, the impact of undetected cases on infection risk within the community remains uncertain. Yang and Wang [20] modeled taking into account the level of pathogens in the reservoir of the environment and their role in the spread of the disease.
Choi and Ki [1] developed a SEIHR (Susceptible, Exposed, Infected, Hospitalized, Recovered) model and estimated the basic reproduction number by the number of confirmed cases reported in Korea.
Sujata and Sumanta [12] studied the impact of the undetected infected persons on the transmission dynamics of COVID-19 for the period 22 March 2020 to 4 May 2020.
Recent studies have advanced the understanding of epidemic models by exploring various incidence rates and treatment functions. Sharma and Sharma [14] investigate the stability of an SIR model incorporating an alert class and modified saturated incidence rate, revealing critical insights into disease dynamics and treatment efficacy. Building on this, Umdekar, Sharma, and Sharma [15] extend the analysis to an SEIR model with similar modifications, highlighting its implications for epidemic control strategies. Additionally, Sharma and Sharma [16] provide a detailed study of an SIQR model with Holling type–II incidence rate, contributing to the broader understanding of model variations and their impacts on disease spread. In 2024, Soni et. al [18] present a comprehensive analysis of prevention strategies for epidemic control using a SEIQHRV (Susceptible, Exposed, Infected, Quarantined, Hospitalized, Recovered, vaccinated) model.

The paper's organization is as follows: Section 2 elaborates on the Methodology, describing the assumptions and notations employed in constructing the model. It also presents the Formulation of the model through diagrams and differential equations. In Section 3, the basic reproduction number of the model is estimated using the next-generation method. Successive sections, namely 4, 5, and 6, delve into the numerical results, main results, and conclusions, respectively.

2. METHODOLOGY

Drawing from prior work by Sujata and Sumanta [12], we expand our model by introducing quarantine and contaminated compartments as innovative components. Employing the next-generation matrix method, we calculate the basic reproduction number. Subsequently, we conduct simulations using MATLAB software to analyze the role of parameters and variables in controlling viral diseases.

2.1. **ASSUMPTION AND NOTATION.**

We make the following assumptions to make our model more realistic.

1. The population distribution is homogeneous so that there are equal chances to contract and propagate the disease.

2. The Entire population is divided into various compartments of the model.

3. Each compartment has some specific property.

4. Susceptible people may become ill after coming in contact with exposed, mild infected, or severely infected people. Also, they may be ill due to contact with the containment surface or area.

5. A part of the susceptible population gets vaccinated and another part does not need to be vaccinated due to inbuilt natural immunity within them.

6. A part of the vaccinated population enters into the susceptible compartment again due to the loss of temporary immunity and another part of the vaccinated population enters into the recovered class due to permanent immunity.

7. Exposed populations is further divided into two infected compartments named as a mildly infected compartment (I_1) and severely infected compartment (I_2). Those in the exposed compartment are asymptomatic carriers and can spread the disease.

8. Population of both infected compartments has equal chances of recovery at a rate γ without the need for any kind of treatment due to the development of natural immunity during the disease period.

9. Populations of both infected compartments get treatment at a rate of σ_1 and σ_2 respectively.

10. Someone in the recovered compartment developed permanent immunity, and was never to be infected again.

11. Quarantined individuals are eligible for treatment and permanent recovery and enter into the recovered compartment at δ rate.

12. Depending upon the severity of infection, exposed or infected individuals can contaminate a non-infected environment that may surge the number of virulent pathogens in the atmosphere.

The following notations were used to build the model:

1. V: Vaccinated population
2. S: Susceptible population
3. E: Exposed population
4. I_1: Infected population, detected through appropriate testing
5. I_2: Undetected Infected population
6. Q: Quarantine population
7. C: Environmental reservoir of the pathogen (i.e. fomites contaminated with coronavirus)
8. R: Recovered population
9. β_e : Rate of transmission between exposed and susceptible persons
10. β_{i_1} : Rate of transmission between susceptible and detected infected persons
11. β_{i_2} : Rate of transmission between susceptible and undetected infected persons
12. β_c : Rate of transmission environment (fomites) to human
13. π : *Influx rate in the population*
14. μ : Natural death rate in the population
15. γ : Rate of the recovery from disease
16. ω : Rate of the death due to disease
17. α^{-1} : Period of incubation
18. β : Percentage of the undetected infected persons
19. σ_1 : Rate of transmission from infected to quarantine compartment

20. σ_2 : Rate of transmission from undetected infected to quarantine compartment
21. η: Rate of removal of the coronavirus from the atmosphere
22. ξ_1: Contribution of exposed persons to the container of the pathogens in the environment
23. ξ_2: Contribution of detected infected persons to the container of the pathogens in the environment
24. ξ_3: Contribution of undetected infected persons to the container of the pathogens in the environment
25. δ: Rate of transmission from quarantine to recovered compartment
26. ψ : Percentage of the susceptible persons who are vaccinated
27. λ : Percentage of the vaccinated persons whose immunity is temporary
28. ρ : Rate at which a susceptible person becomes vaccinated
29. κ : Rate at which vaccinated person lose their immunity

2.2. **FORMULATION OF THE MODEL.** In our VSEIQCR model (See Figure 1), we distributed the total human populations into seven compartments- vaccinated (V), susceptible (S),exposed (E), infected detected I_1, infected undetected I_2, quarantined (Q) and recovered (R). Now, we have introduced an additional compartment (C) for the environmental container of the coronavirus pathogen, which contributes to the spread of the infection.

$$\frac{dS}{\mathrm{dt}} = \pi - \beta_e SE - \beta_{i_1} SI_1 - \beta_{i_2} SI_2 - \beta_c SC - (\mu + \rho)S + \lambda\kappa V$$

$$\frac{dE}{\mathrm{dt}} = \beta_e SE + \beta_{i_1} SI_1 + \beta_{i_2} SI_2 + \beta_c SC - (\mu + \alpha)\, E$$

$$\frac{dI_1}{\mathrm{dt}} = \alpha\beta E - (\mu + \omega + \gamma + \sigma_1)\, I_1$$

$$\frac{dI_2}{\mathrm{dt}} = \alpha\,(1 - \beta)\, E - (\mu + \omega + \gamma + \sigma_2)\, I_2$$

$$\frac{\mathrm{dC}}{\mathrm{dt}} = \xi_1 E + \xi_2 I_1 + \xi_3 I_2 - \eta C$$

$$\frac{\mathrm{dQ}}{\mathrm{dt}} = \sigma_1 I_1 + \sigma_2 I_2 - (\mu + \delta)\, Q$$

$$\frac{\mathrm{dR}}{\mathrm{dt}} = (I_1 + I_2)\,\gamma + \delta Q + \rho\,(1 - \psi)\, S + \kappa\,(1 - \lambda)\, V - \mu R$$

$$\frac{\mathrm{dV}}{\mathrm{dt}} = \rho\psi S - (\mu + \kappa)\, V$$

Obviously, the system of equations has a disease-free equilibrium, $X_{\mathrm{DFE}} = \left(\frac{\pi}{\mu+\rho}\ ,\ 0,\ 0, 0, 0, 0, 0, 0\right)$.

3. THE BASIC REPRODUCTION NUMBER

The basic reproduction number is the measurement of a disease's potential spread. It represents the average number of secondary infections caused by a single infectious person in a completely susceptible population. This number indicates whether a disease will die out or persist in the population. Specifically, $R_0 < 1$ implies that the disease will eventually die out, while $R_0 \geq 1$ suggests that the disease will continue to affect the population over time. Soni et al. [17] investigate the basic reproduction number R_0 and herd immunity for COVID-19 in India, emphasizing their critical

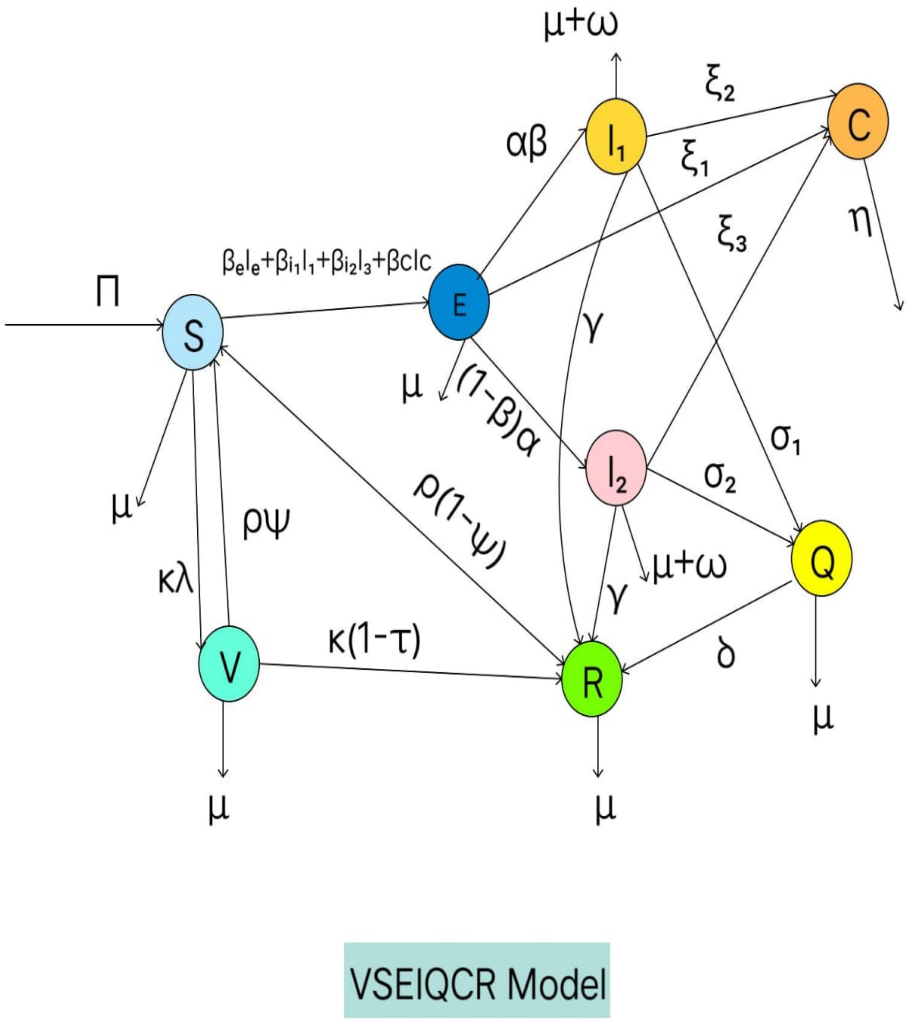

FIGURE 1. VSEIQCR Model

relationship. The study highlights how R_0 , a measure of disease transmission potential, directly influences the threshold for achieving herd immunity.
We derive this number with the help of next-generation method given by Van den Driessche [19]. This method separates the compartments into infected compartment (E, I_1, I_2, C) and uninfected compartments (V, S, Q, R). x and y denote the vector of variables in the infected and the non-infected compartments i.e. $x = (x_1, x_2, x_3, x_4)$ and $y = (y_1, y_2, y_3, y_4)$ where $(x_1, x_2, x_3, x_4, y_1, y_2, y_3, y_4)$ represent the $E, I_1, I_2, C, S, Q, R, V$ compartments respectively. The dynamical system of equations may be written as:

$$x_1^{'} = F_1(x, y) = \beta_e SE + \beta_{i1} SI_1 + \beta_{i2} SI_2 + \beta_c SC - (\mu + \alpha) E,$$

$$x_2^{'} = F_2(x, y) = \alpha\beta E - (\mu + \omega + \gamma + \sigma_1) I_1,$$

$$x_3^{'} = F_3(x,y) = \alpha(1-\beta)E - (\mu+\omega+\gamma+\sigma_2)I_2,$$

$$x_4^{'} = F_4(x,y) = \xi_1 E + \xi_2 I_1 + \xi_3 I_2 - \eta C,$$

$$y_1^{'} = G_1(x,y) = \pi - \beta_e SE - \beta_{i1} SI_1 - \beta_{i2} SI_2 - \beta_c SC - \mu S - (\mu+\rho)S + \lambda\kappa V,$$

$$y_2^{'} = \sigma_1 I_1 + \sigma_2 I_2 - (\mu+\delta)Q,$$

$$y_3^{'} = (I_1+I_2)\gamma + \delta Q + \rho(1-\psi)S + \kappa(1-\lambda)V - \mu R,$$
$$y_4^{'} = \rho\psi S - (\mu+\kappa)V,$$

Now, we divide the infection compartments right hand side as shown below:

$X_i^{'} = M_i(x,y) - N_i(x,y)\ \forall\ i = 1,\ 2,\ 3,\ 4.$ where $M_i(x,y)$ is the rate of new infection in the compartment x_i ($\forall\ i = 1,\ 2,\ 3,\ 4$) and $N_i(x,y)$ represent the other transitory terms of infected compartment.

$$\begin{aligned}
&M_1(x,y) = \beta_e SE + \beta_{i1} SI_1 + \beta_{i2} SI_2 + \beta_c SC - (\mu+\alpha)E, && N_1(x,y) = 0,\\
&M_2(x,y) = 0, && N_2(x,y) = -\alpha\beta E + (\mu+\omega+\gamma+\sigma_1)I_1,\\
&M_3(x,y) = 0, && N_3(x,y) = -\alpha(1-\beta)E + (\mu+\omega+\gamma+\sigma_2)I_2,\\
&M_4(x,y) = 0, && N_4(x,y) = -\xi_1 E - \xi_2 I_1 - \xi_3 I_2 + \eta C.
\end{aligned}$$

The linearized system of infected compartments may be written as:

$$x_i^{'} = (F-T)x,$$

where, F and T are the infections and the transition matrices respectively.

$$F = \left[\frac{\partial M_i}{\partial x_j}\right],$$
$$T = \left[\frac{\partial N_i}{\partial x_j}\right].$$

which arise from linearizing the system around the disease-free equilibrium.

$$F = \begin{bmatrix} \beta_e S_0 & \beta_{i_1} S_0 & -\beta_{i_2} S_0 & \beta_c S_0 \\ 0 & 0 & 0 & 0 \\ 0 & 0 & 0 & 0 \\ 0 & 0 & 0 & 0 \end{bmatrix},$$

$$T = \begin{bmatrix} \alpha+\mu & 0 & 0 & 0 \\ -\alpha\beta & \mu+\omega+\gamma+\sigma_1 & 0 & 0 \\ -\alpha(1-\beta) & 0 & \mu+\omega+\gamma+\sigma_2 & 0 \\ -\xi_1 & -\xi_2 & -\xi_3 & \eta \end{bmatrix}.$$

The next-generation matrix is defined as

$$D = FT^{-1}.$$

The basic reproduction number $\mathbb{R}_0$ for the model (1) is determined by the spectral radius of the next-generation matrix D and is given by: $\mathbb{R}_0 = R_1 + R_2 + R_3 + R_4$, where

$$R_1 = \frac{\beta_e \pi}{(\mu+\alpha)(\mu+\rho)},$$

$$R_2 = \frac{\beta_{i1}\alpha\beta\pi}{(\mu+\alpha)(\mu+\rho)(\mu+\omega+\gamma+\sigma_1)},$$

$$R_3 = \frac{\beta_{i2}\alpha(1-\beta)\pi}{(\mu+\alpha)(\mu+\rho)(\mu+\omega+\gamma+\sigma_2)},$$

$$R_4 = \frac{\beta_c\pi\{\alpha\beta(\mu+\omega+\gamma+\sigma_2)\xi_2 + \alpha\xi_3(1-\beta)(\mu+\omega+\gamma+\sigma_1) + \xi_1(\mu+\omega+\gamma+\sigma_1)(\mu+\omega+\gamma+\sigma_2)\}}{(\mu+\alpha)(\mu+\omega+\gamma+\sigma_1)(\mu+\omega+\gamma+\sigma_2)(\mu+\rho)\eta}$$

,

where R_1, R_2, R_3, *and* R_4 *provide the evaluation of the risk of disease by pathways S to E, S to* I_1, *S to* I_2 *compartment and from environment to human respectively.*

4. LOCAL STABILITY AT DISEASE FREE EQUILIBRIUM

The Jacobean matrix of the model is given by:

$$J = \begin{bmatrix} -\Delta_1-\rho & -\beta_e & -\beta_{i_1} & -\beta_{i_2} & -\beta_c & 0 & 0 & \lambda\kappa \\ -\Delta_1 & -(\mu+\alpha) & 0 & 0 & 0 & 0 & 0 & 0 \\ 0 & \alpha\beta & -(\mu+\omega+\gamma+\sigma_1) & 0 & 0 & 0 & 0 & 0 \\ 0 & \alpha(1-\beta) & 0 & -(\mu+\omega+\gamma+\sigma_2) & 0 & 0 & 0 & 0 \\ 0 & \xi_1 & \xi_2 & \xi_3 & -\eta & 0 & 0 & 0 \\ 0 & 0 & \sigma_1 & \sigma_2 & 0 & -(\mu+\delta) & 0 & 0 \\ \rho(1-\psi) & 0 & \gamma & \gamma & 0 & \delta & -\mu & \kappa(1-\lambda) \\ \rho\psi & 0 & 0 & 0 & 0 & 0 & 0 & -(\mu+\kappa) \end{bmatrix},$$

where $\Delta_1 = \beta_e E + \beta_{i1} I_1 + \beta_{i2} I_2 + \beta_c C$.

At the point X_{DFE} the Jacobean matrix of the model is given by:

$$J_{X_{DFE}} = \begin{bmatrix} -\rho & -\beta_e & -\beta_{i_1} & -\beta_{i_2} & -\beta_c & 0 & 0 & \lambda\kappa \\ 0 & -(\mu+\alpha) & 0 & 0 & 0 & 0 & 0 & 0 \\ 0 & \alpha\beta & -(\mu+\omega+\gamma+\sigma_1) & 0 & 0 & 0 & 0 & 0 \\ 0 & \alpha(1-\beta) & 0 & -(\mu+\omega+\gamma+\sigma_2) & 0 & 0 & 0 & 0 \\ 0 & \xi_1 & \xi_2 & \xi_3 & -\eta & 0 & 0 & 0 \\ 0 & 0 & \sigma_1 & \sigma_2 & 0 & -(\mu+\delta) & 0 & 0 \\ \rho(1-\psi) & 0 & \gamma & \gamma & 0 & \delta & -\mu & \kappa(1-\lambda) \\ \rho\psi & 0 & 0 & 0 & 0 & 0 & 0 & -(\mu+\kappa) \end{bmatrix}$$

Using MATLAB software and the parameter values outlined in the table 1, we evaluated the eigenvalues at the disease-free equilibrium X_{DFE}.

Our analysis revealed that all eigenvalues at this equilibrium have negative real parts (i.e. $-0.73, -0.7997, -0.9, -0.8543, -0.2, -1.515, -1.015, -7.7$). According to the Routh-Hurwitz criterion, this result confirms local asymptotic stability when the basic reproductive number $\mathbb{R}_0$ is less than 1, and indicates instability when it exceeds 1.

5. GLOBAL STABILITY AT DISEASE FREE EQUILIBRIUM

To investigate the global stability of the disease-free equilibrium (DFE) in our model, we conducted a numerical simulation based on the set of differential equations governing the system. The value of $\mathbb{R}_0$ depends on each of its component. Given the provided parameter values in the table 1, we compute the basic reproduction number $\mathbb{R}_0$ and its components $\mathbb{R}_1, \mathbb{R}_2, \mathbb{R}_3, and \mathbb{R}_4$. $\mathbb{R}_1 = 1.2483 \times 10^{-6}, \mathbb{R}_2 = 5.7468 \times 10^{-7}, \mathbb{R}_3 = 1.1020 \times 10^{-7}, \mathbb{R}_4 = 2.9339 \times 10^{-8}$. Thus, the basic reproduction number is: $\mathbb{R}_0 = 1.9625 \times 10^{-6}$. This value of $\mathbb{R}_0$ being much less than 1 confirms that the disease-free equilibrium (DFE) is globally stable, the disease will not spread in the population, and the system will return to the DFE over time. We use the values in table 1 with $S_0 = 70,000$, $E_0 = 50,000$, $I_{1_0} = 3,0,000$, $I_{2_0} = 4,0,000$, $C_0 = 5000$, $Q_0 = 25,000$, $V_0 = 30,000$, and $R_0 = 50,000$ to perform a simulation for the Disease-Free Equilibrium (DFE), as shown in figure 2.

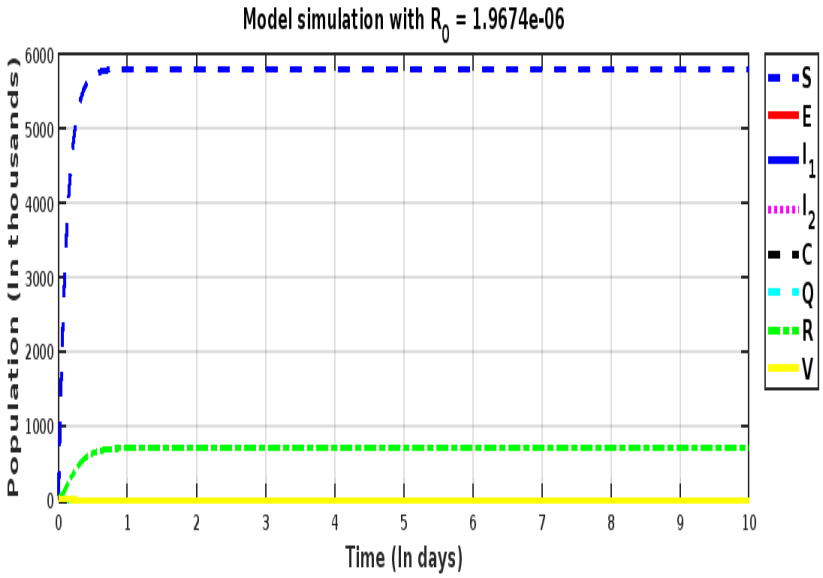

FIGURE 2. DFE

The simulation results, depicted in figure 2, demonstrate the temporal evolution of each compartment within the model. Over the course of the simulation:

1. Susceptible Population (S): The susceptible population stabilizes near the value $\frac{\pi}{\mu+\rho}$, consistent with the DFE. This behavior indicates that the introduction of disease-related perturbations does not significantly deplete the susceptible population, maintaining its stability.
2. Exposed (E), Infected I_1 and I_2: The exposed and infected populations, both I_1 and I_2, consistently approach zero as time progresses. This outcome suggests that the infection does not sustain itself within the population and tends to die out, leading to a return to the disease-free state.
3. Contaminated Carrier (C) and Quarantined (Q): Similar to the exposed and infected populations, the carrier and quarantined compartments also trend towards zero. This further reinforces the notion that the disease cannot persist within the population under the given parameters.

4. Recovered (R) and Vaccinated (V): The recovered and vaccinated populations stabilize at levels that do not interfere with the overall disease dynamics, thus supporting the DFE stability.

These results collectively confirm the global stability of the disease-free equilibrium within the context of our model. The simulations reveal that irrespective of initial conditions, the system invariably returns to the DFE over time, thereby affirming the robustness of this equilibrium. The observed stability is consistent across all simulated scenarios, indicating that the model effectively captures the mechanisms necessary for disease eradication under the given parameters.

Furthermore,to establish global stability at the DFE, we propose the following Lyapunov function:

$$V(S,E,I_1,I_2,C,Q,R,V) = \frac{1}{2}\left(\frac{S-S^*}{S^*}\right)^2 + \frac{E}{\mu+\alpha} + \frac{I_1}{\mu+\omega+\gamma+\sigma_1} + \frac{I_2}{\mu+\omega+\gamma+\sigma_2}$$

where $S^* = \frac{\pi}{\mu+\rho}$.

Time Derivative of the Lyapunov Function. The time derivative of $V(S,E,I_1,I_2,C,Q,R,V)$ is computed as follows:

$$\frac{dV}{dt} = \frac{\partial V}{\partial S}\frac{dS}{dt} + \frac{\partial V}{\partial E}\frac{dE}{dt} + \frac{\partial V}{\partial I_1}\frac{dI_1}{dt} + \frac{\partial V}{\partial I_2}\frac{dI_2}{dt}$$

where the partial derivatives are:

$$\frac{\partial V}{\partial S} = \frac{S-S^*}{S^{*2}}$$

$$\frac{\partial V}{\partial E} = \frac{1}{\mu+\alpha}, \quad \frac{\partial V}{\partial I_1} = \frac{1}{\mu+\omega+\gamma+\sigma_1}, \quad \frac{\partial V}{\partial I_2} = \frac{1}{\mu+\omega+\gamma+\sigma_2}$$

Substituting the derivatives from the system:

$$\frac{dV}{dt} = \frac{S-S^*}{S^{*2}}\left(\pi - \mu S - \rho S + \lambda\kappa V - \beta_e SE - \beta_{i1} SI_1 - \beta_{i2} SI_2 - \beta_c SC\right)$$

$$+\frac{\beta_e SE + \beta_{i1} SI_1 + \beta_{i2} SI_2 + \beta_c SC - (\mu+\alpha)E}{\mu+\alpha}$$

$$+\frac{\alpha\beta E - (\mu+\omega+\gamma+\sigma_1)I_1}{\mu+\omega+\gamma+\sigma_1}$$

$$+\frac{\alpha(1-\beta)E - (\mu+\omega+\gamma+\sigma_2)I_2}{\mu+\omega+\gamma+\sigma_2}$$

Given the structure of $\frac{dV}{dt}$, the following conclusions can be drawn:

Near the DFE: Since $S \approx S^*$ and all other compartments E, I_1, I_2 are small or zero, $V(S,E,I_1,I_2,C,Q,R,V)$ is positive and $\frac{dV}{dt} \leq 0$. This indicates that the Lyapunov function does not increase over time, with equality only at the DFE.

Global Behavior: If $\frac{dV}{dt}$ is negative semi-definite, and the only equilibrium where V is minimized is the DFE, then the system will asymptotically approach the DFE regardless of the initial conditions, provided they are in the feasible region. To demonstrate that $\frac{dV}{dt}$ is negative semi-definite and that the only equilibrium where V is minimized is the Disease-Free Equilibrium (DFE), we analyze the sign of each term in the expression for $\frac{dV}{dt}$.

First Term:

$$\frac{S - S^*}{S^{*2}} (\pi - \mu S - \rho S + \lambda \kappa V - \beta_e SE - \beta_{i1} SI_1 - \beta_{i2} SI_2 - \beta_c SC)$$

$S - S^*$ changes sign depending on whether $S > S^*$ or $S < S^*$. The expression inside the parentheses represents the change in S over time. In the DFE, $S = S^*$ and the terms involving infected compartments (E, I_1, I_2, C) are zero.

Second Term:

$$\frac{\beta_e SE + \beta_{i1} SI_1 + \beta_{i2} SI_2 + \beta_c SC - (\mu + \alpha)E}{\mu + \alpha}$$

This term represents the change in E. At DFE, $E = 0$ and the entire term becomes zero. - Outside DFE, this term is positive when there is transmission but negative when the removal rate $(\mu + \alpha)$ dominates.

Third Term:

$$\frac{\alpha\beta E - (\mu + \omega + \gamma + \sigma_1) I_1}{\mu + \omega + \gamma + \sigma_1}$$

At DFE, $I_1 = 0$, $E = 0$, so this term is zero. Otherwise, this term can be positive or negative depending on the balance between infection (first term) and removal (second term).

Fourth Term:

$$\frac{\alpha(1 - \beta)E - (\mu + \omega + \gamma + \sigma_2) I_2}{\mu + \omega + \gamma + \sigma_2}$$

Similar analysis to the third term. At DFE, $I_2 = 0$, $E = 0$, and the term is zero.

At the DFE, where $E = 0$, $I_1 = 0$, $I_2 = 0$, $C = 0$, $Q = 0$, and $S = S^*$:

$$\frac{dV}{dt} = 0$$

For non-DFE equilibria, $\frac{dV}{dt} \leq 0$. The term $\frac{S - S^*}{S^{*2}}$ multiplied by the expression involving infections is negative because infections reduce susceptible individuals. Similarly, the terms involving E, I_1, and I_2 become negative when infected compartments are non-zero, reflecting the progression of disease and recovery or removal of infected individuals.

$\frac{dV}{dt}$ is negative semi-definite, indicating that V does not increase over time and decreases whenever there are infected individuals. The only point where $\frac{dV}{dt} = 0$ and V reaches its minimum is at the Disease-Free Equilibrium (DFE), where all compartments except S are zero. This demonstrates that the system stabilizes at the DFE, where no infection persists.

We find that the entire population will eventually consist only of susceptible, vaccinated, or recovered individuals and the Lyapunov function ensures that even if the disease initially spreads through the population, the natural dynamics of the system will drive the population back to the disease-free equilibrium, where the disease cannot persist. Thus, this analysis guarantees that, under the given model and assumptions, the disease will not become endemic or persist in the long run; instead, it will fade out, leaving the population disease-free. Therefore, the disease-free equilibrium $X_{\text{DFE}} = \left(\frac{\pi}{\mu + \rho}, 0, 0, 0, 0, 0, 0, 0\right)$ is globally asymptotically stable.

6. NUMERICAL RESULTS

We estimated the basic reproduction number for the period from 16 January 2021 to 28 February 2021. After starting of the vaccination program in India, we eagerly want to know the impact of undetected infected persons on the transmission dynamics of COVID-19. As of 16 January 2020, the cumulative confirmed cases, death cases and recovered cases were 10558637, 151720 and 10196056 respectively, whereas on 28 February 2020, these data became 11111978, 156603 and 10784401 respectively. Because, those who are exposed and Undetected tend to live in the community, they can spread the disease at the same rate [13].

Also, the family members impacted by COVID-19 may survive in the environment from a couple of hours to several days [20]. In this study, this value was taken as 5 hours and, consequently, the elimination rate of virus is 0.2 per day. We estimated the recovery rate (γ) as follows- $\frac{\text{Difference of cumulative recovered}}{\text{Difference of cumulative confirmed}} * \frac{1}{\text{Average recovery time in days}} = \frac{10784401-10196056}{11111978-10558637} * \frac{1}{14} = 0.075$ *per day*. As of 1 January 2021, the total estimated population of India was 1,390,537,387 [3].

TABLE 1. **Parameter Estimates**

S.No.	Parameter	Estimated Value	Sources
1	π	47964 per day	[3]
2	β_e	$0.25 \times 0.1231 \times 10^{-7}$	[13]
3	β_{i_1}	$0.25 \times 0.5944 \times 0.1231 \times 10^{-7}$	[13]
4	β_{i_2}	$0.25 \times 0.1231 \times 10^{-7}$	[13]
5	β_c	1.03×10^{-8}	[13]
6	μ	7.344 per day	[4]
7	γ_1, γ_2	0.075 per day	Estimated
8	ω	0.01	Estimated
9	α	7 days	[20]
10	β	0.9	[13]
11	σ_1, σ_2	$0.7, 0.2$	Assumed
12	η	0.2	[12]
13	ξ_1	0.001	[13]
14	ξ_2	0.000398	[13]
15	ξ_3	0.001	[13]
16	δ	0.1243	[10]
17	ψ	0.008	Assumed
18	λ	0.05	Assumed
19	ρ	0.9	Assumed
20	κ	0.07	Assumed

In the below table 2, we estimated the contribution of exposed individuals, undetected infected individuals, detected infected individuals, and contaminated pathogens in the final reproduction number. We vary the values of the transmission rate (ρ) and percentage of undetected infected individuals ($1-\beta$) simultaneously, to check the impact of undetected infected and vaccinated individuals on the transmission of epidemic COVID-19.

As $(1-\beta)$ increases from 0.1 to 0.4, the overall risk R_0 (which is the sum of all individual risks) slightly increases. This trend suggests that as a smaller proportion of the population remains immune (i.e., $(1-\beta)$ increases), the total risk of disease

TABLE 2. **Results for Different Values of ρ**

S.No.	$(1-\beta)$	$\mathbf{R_1}$	$\mathbf{R_2}$	$\mathbf{R_3}$	$\mathbf{R_4}$	$\mathbf{R_0}$
When $\rho = 0.9$						
1	0.1	1.2483e-06	5.7503e-07	1.1453e-07	2.9553e-08	1.9674e-06
2	0.2	1.2483e-06	5.1113e-07	2.2907e-07	3.0589e-08	2.0191e-06
3	0.3	1.2483e-06	4.4724e-07	3.4360e-07	3.1625e-08	2.0707e-06
4	0.4	1.2483e-06	3.8335e-07	4.5814e-07	3.2661e-08	2.1224e-06
When $\rho = 0.8$						
1	0.1	1.2636e-06	5.8209e-07	1.1594e-07	2.9916e-08	1.9915e-06
2	0.2	1.2636e-06	5.1741e-07	2.3188e-07	3.0965e-08	2.0438e-06
3	0.3	1.2636e-06	4.5273e-07	3.4782e-07	3.2013e-08	2.0962e-06
4	0.4	1.2636e-06	3.8806e-07	4.6376e-07	3.3062e-08	2.1485e-06

transmission also increases. The risk via the pathway from susceptible to exposed individuals (R_1) is the largest contributor to the total risk R_0, highlighting that the initial exposure is the most critical phase in disease spread.

The risks associated with the pathways to detected infected individuals (R_2), undetected infected individuals (R_3), and environmental transmission (R_4) are smaller, but they do increase as $(1-\beta)$ increases. Comparing $\rho = 0.9$ and $\rho = 0.8$, the risks R_1, R_2, R_3, and R_4 are slightly higher when $\rho = 0.8$ than when $\rho = 0.9$. This indicates that a lower ρ leads to an increased overall risk of disease transmission.

The data show that reducing the proportion of the immune population ($(1-\beta)$) results in a higher overall risk of disease transmission. The most significant risk occurs at the initial stage (from susceptible to exposed individuals). Hence, strategies to minimize disease transmission should focus on enhancing immunity and maintaining or improving vaccination.

Additionally, the risk R_2 associated with detected infected individuals (I_1) is consistently higher than R_3 associated with undetected infected individuals (I_2) across all values of $(1-\beta)$ and both ρ values, suggesting that detected infected individuals pose a greater risk to disease spread, possibly due to more interactions or higher infectiousness. The smaller increase in R_3 suggests that undetected infected individuals contribute less to transmission risk relative to detected cases.

We can easily observe that in both the cases (when $\rho = 0.9$ or when $\rho = 0.8$) whenever the number of undetected infected individuals is 0.1, 0.2, and 0.3 percent, the dominant part of disease risk is detected infected compartment, whereas, whenever its value is 0.4 percent the undetected infected individuals compartment contribution dominantly in the risk of disease spread. In this context, the contribution of $\mathbb{R}_4$ in the total basic reproduction number cannot be neglected.

As $(1-\beta)$ increases, R_4 shows a slight increase, suggesting that as more individuals become susceptible, fomite transmission risk also rises, though less significantly than other pathways. When ρ decreases, R_4 values increase slightly, similar to other risks, but still remain minor compared to direct transmission routes. This highlights that while environmental hygiene and disinfection are important, the primary focus for

controlling disease spread should be on direct transmission routes and improving immunity in the population.

6.1. **EFFECT OF PARAMETERS ON INFECTED COMPARTMENT.** We set $\beta_e = 0.3 \times 10^{-5}$, $\beta_{i_1} = 0.3 \times 10^{-2}$, $\beta_{i_2} = 0.3 \times 10^{-2}$, and $\beta_c = 0.5 \times 10^{-6}$, while keeping the remaining parameters the same as listed in Table 1. This setup is used to perform a simulation to assess the effect of a particular parameter on various infected compartments. For the simulation, we initialize with $S_0 = 70,000$, $E_0 = 50,000$, $I_{1_0} = 3,0,000$, $I_{2_0} = 4,0,000$, $C_0 = 5000$, $Q_0 = 25,000$, $V_0 = 30,000$, and $R_0 = 50,000$ to perform simulation.

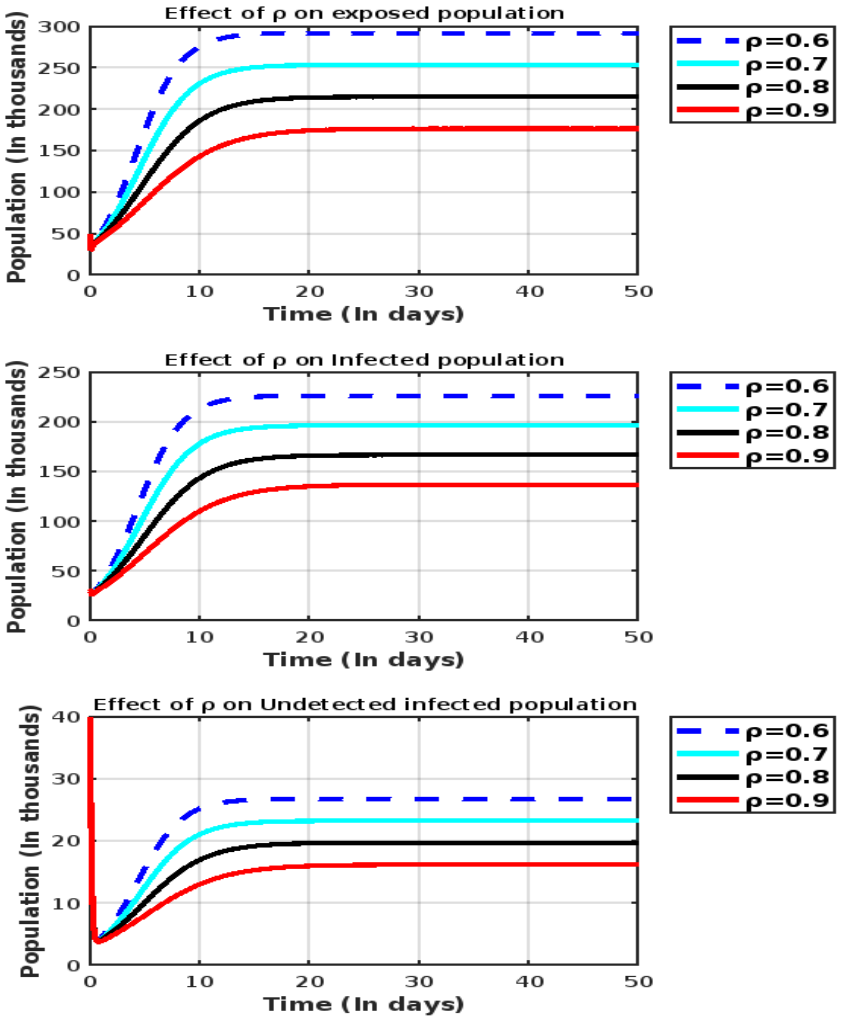

FIGURE 3. Effect of ρ

In Figure 3, as the vaccination rate ρ of susceptible individuals increases, all the curves corresponding to the infected compartments show a decline in their populations.

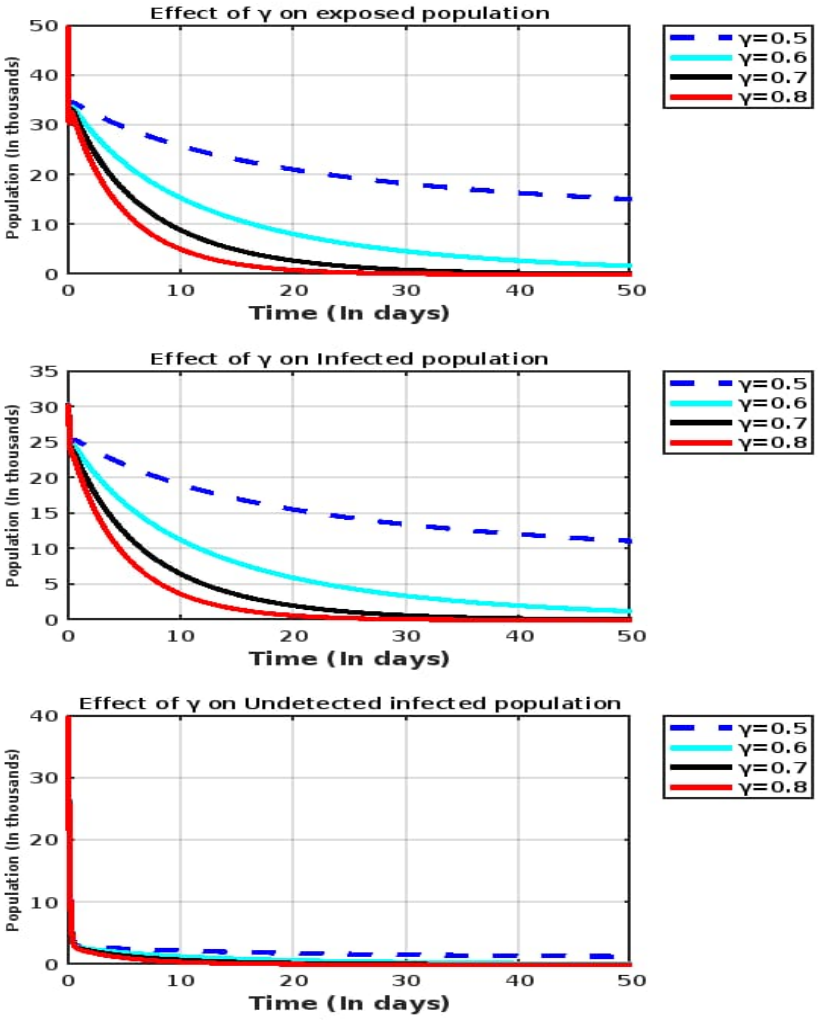

FIGURE 4. Effect of γ

In Figure 4, as the recovery rate of infected individuals γ increases, all the curves corresponding to the infected compartments show a decline in their populations.

In Figure 5, as the percentage of undetected infected populations β decreases, all the curves corresponding to the infected compartments show a decline in their populations.

In Figure 6, as the quarantine rate σ_1 of infected individuals increases, all the curves corresponding to the infected compartments show a decline in their populations.

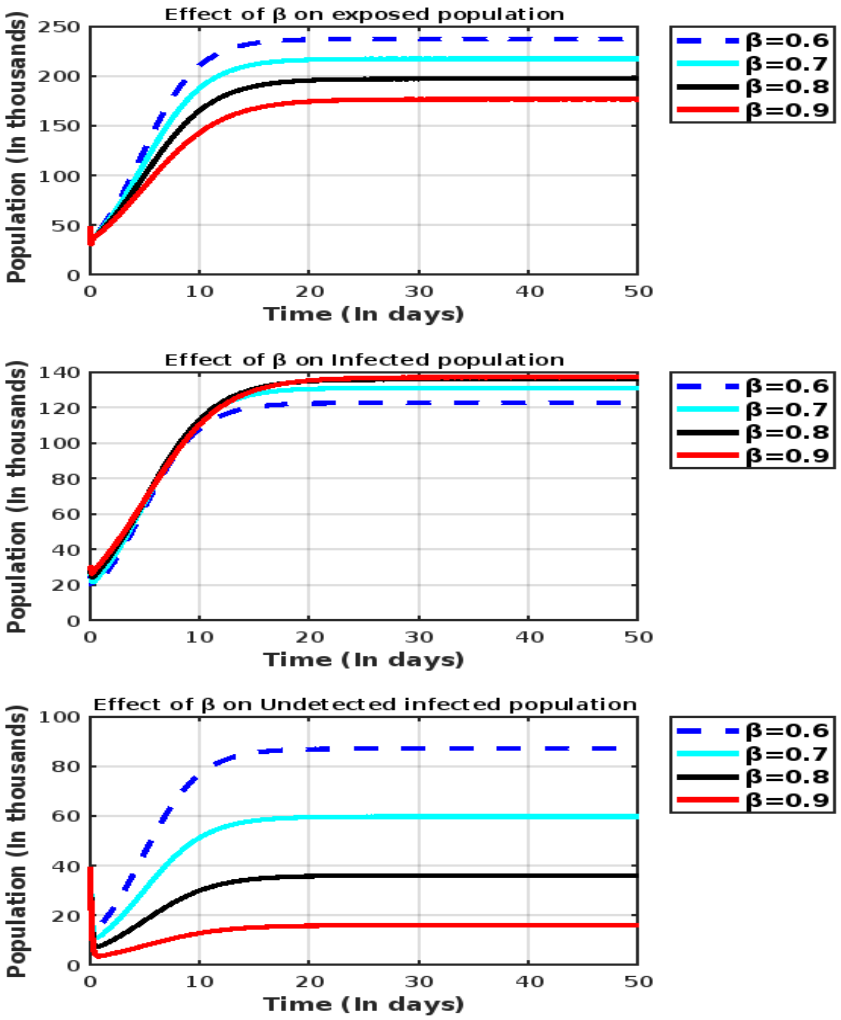

FIGURE 5. Effect of β

In Figure 7, as the quarantine rate σ_2 of undetected infected individuals increases, all the curves corresponding to the infected compartments show a decline in their populations.

In Figure 8, as the transmission rate β_{i_1} decreases, all the curves corresponding to the infected compartments show a decline in their populations.

In Figure 9, as the transmission rate β_{i_2} decreases, all the curves corresponding to the infected compartments display a decline in their populations.

In Figure 10, as the transmission rate β_e decreases, all the curves corresponding to the infected compartments display a decline in the corresponding populations.

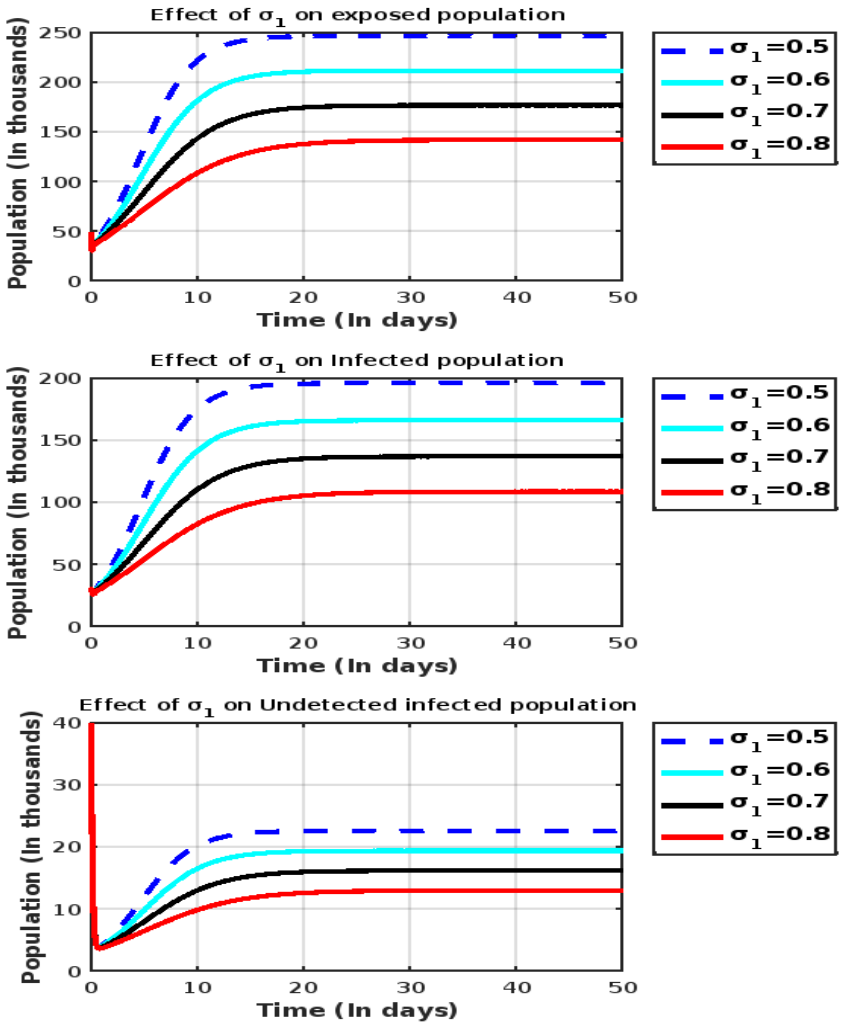

FIGURE 6. Effect of σ_1

7. MAIN RESULTS

According to the World Health Organization (WHO) [5], individuals susceptible to infection may contract the virus through contact with contaminated objects or surfaces, known as fomites. Before cleansing their hands, these individuals may inadvertently touch their eyes, mouth, or nose, thereby facilitating transmission. Therefore, the role of fomites in COVID-19 transmission is a crucial aspect addressed in our study. Mitigation strategies include frequent hand washing and sanitization, as well as the consistent use of masks as preventive measures.

Moreover, exposed and undetected infected individuals contribute to the spread of COVID-19 unknowingly. Thus, it is important to detect, isolate, and treat them.

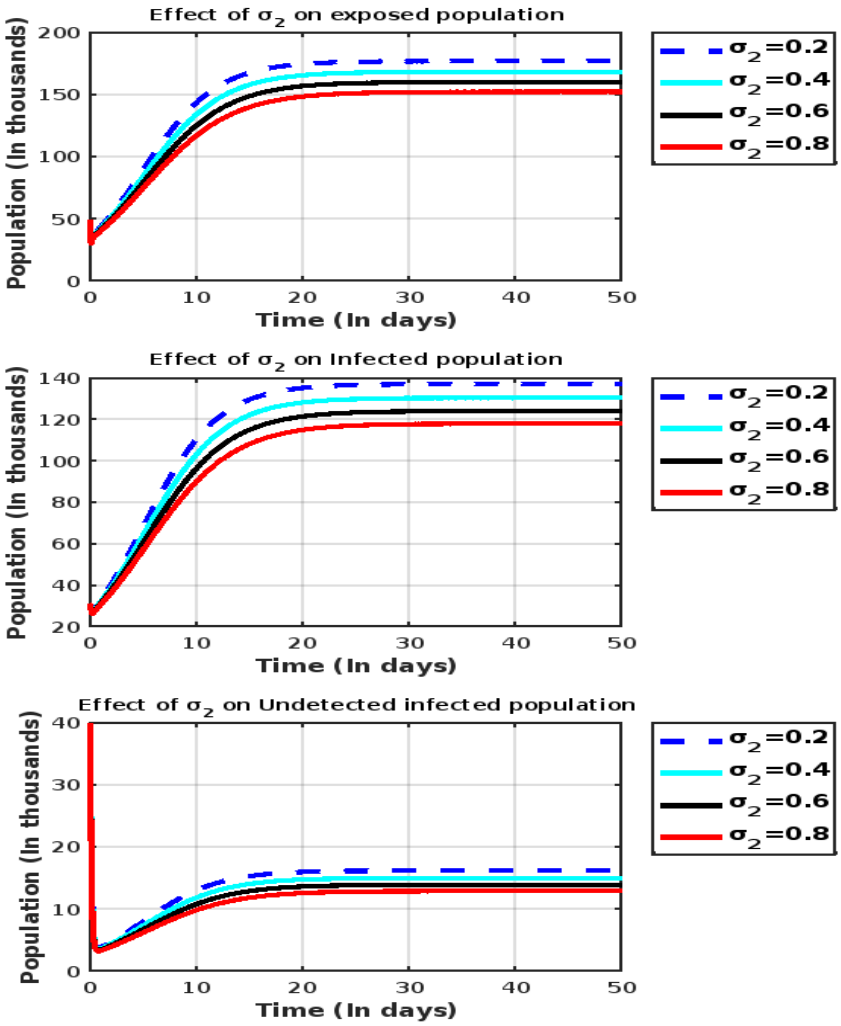

FIGURE 7. Effect of σ_2

This underscores the significance of tracing and testing to prevent the spread of the disease. Even though vaccines are available to control and reduce the risk of infection, undetected infected individuals still significantly contribute to the basic reproduction number. Hence, detecting and isolating these individuals can help prevent the spread of infection.

Furthermore, it is necessary to decrease the risk of spread by increasing the percentage of vaccinated people. Some individuals may lose their immunity due to a low immune response against the disease, so it is important for people to complete both vaccine doses. They should follow the guidelines issued by the Government of India and should not neglect preventive precautions. Our study may be the first to simultaneously include fomites, quarantine, undetected infected individuals,

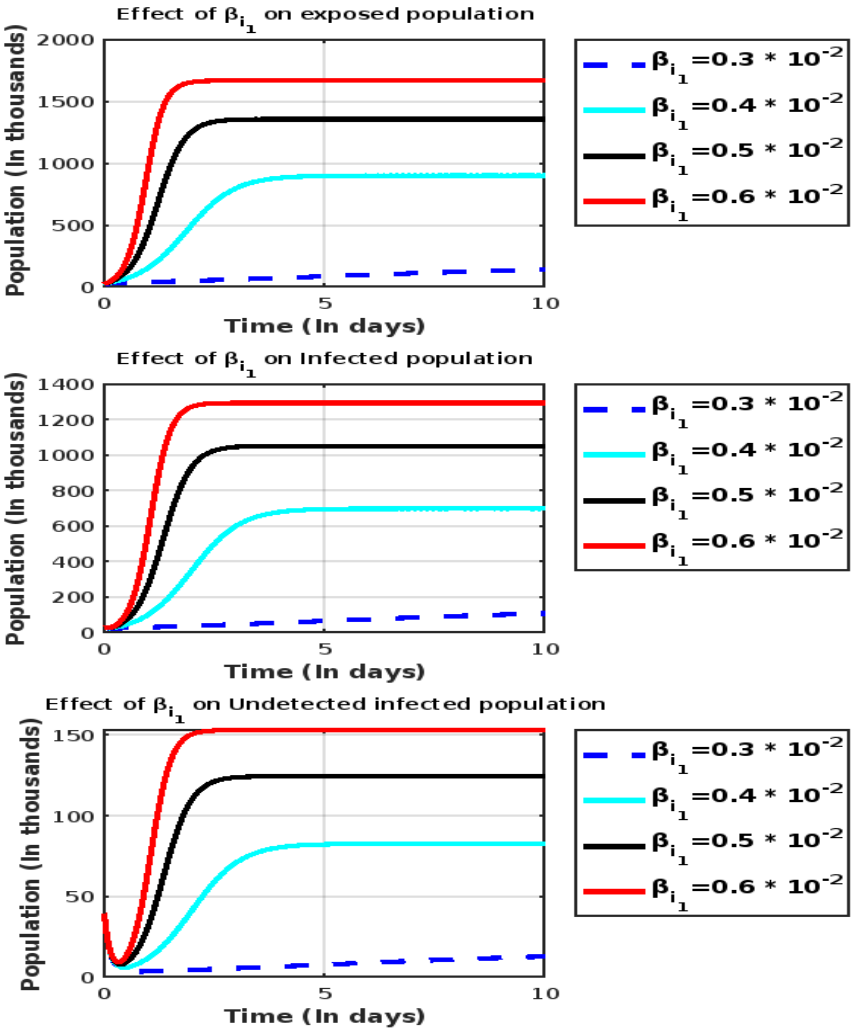

FIGURE 8. Effect of β_{i_1}

and vaccinated individuals in a mathematical model of COVID-19 transmission within the population. The estimation of the basic reproduction number is based on parameter values selected from other relevant studies; therefore, our findings may differ from the original values.

8. CONCLUSIONS

The risk of COVID-19 spread increases with the rise in undetected infected cases. Additionally, carelessness and lack of awareness regarding fomite transmission significantly contribute to the persistence of the disease within the population. Since undetected

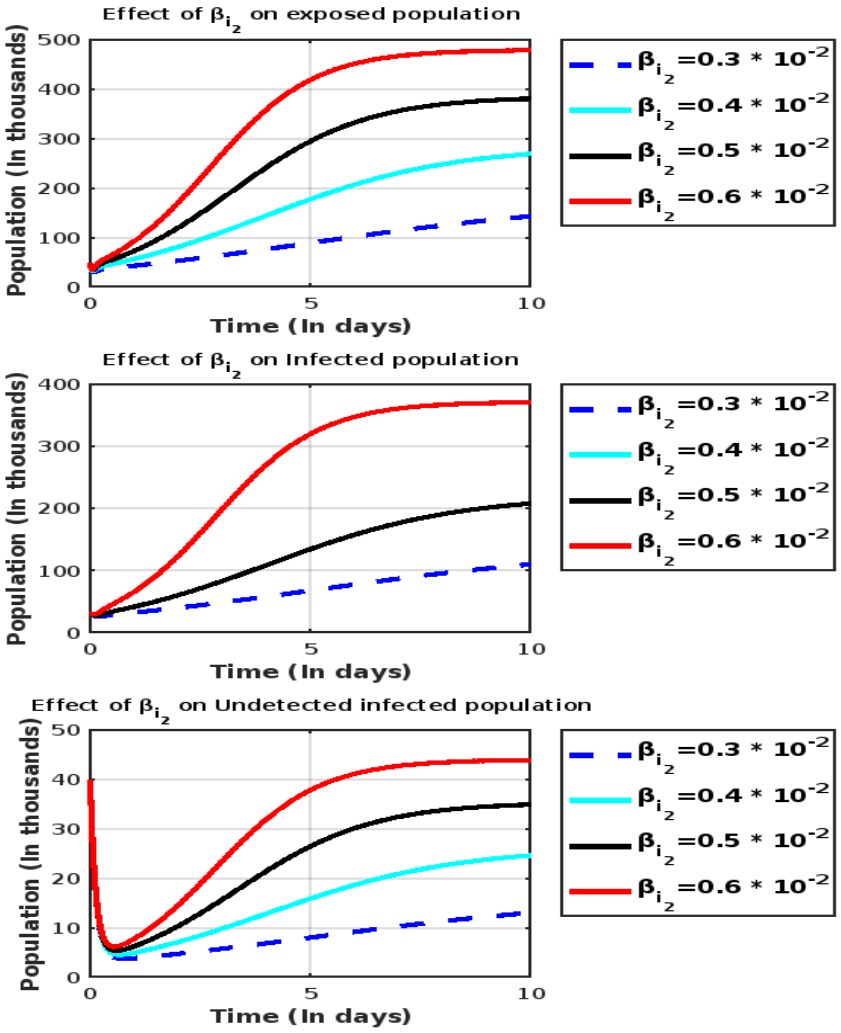

FIGURE 9. Effect of β_{i2}

infected and exposed individuals unknowingly spread the virus, it is crucial to identify, isolate, and treat them to prevent further transmission.

REFERENCES

1. S. Choi, M. Ki, Estimating the Reproductive Number and the Outbreak Size of COVID-19 in Korea. Epidemiology and Health, 42, (2020). https://doi.org/10.4178/epih.e2020011.
2. Director, W. H. O. General's Opening Remarks at the Media Briefing on COVID-19-11 March 2020. World Health Organization (2020).
3. Countrymeters. (2021, November 1). India population. Countrymeters. https://countrymeters.info/en/India.
4. MacroTrends. (2021, November 1). India death rate. MacroTrends, https://www.macrotrends.net/countries/IND/india/death-rate.

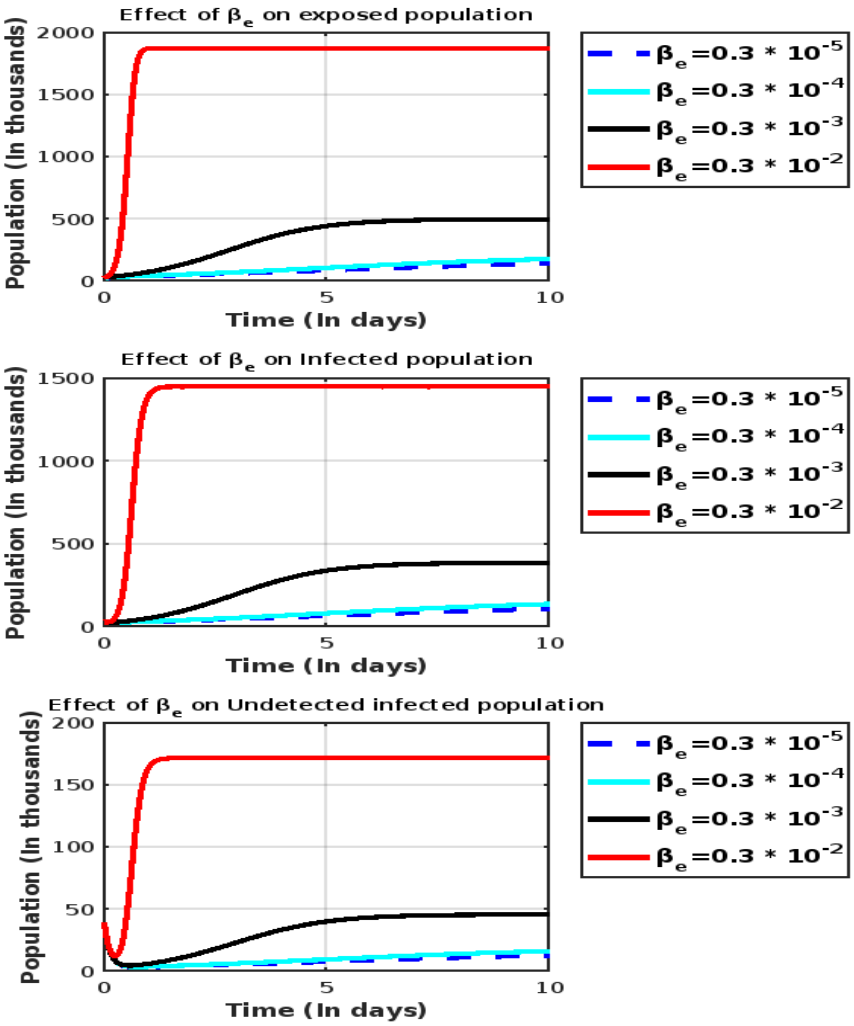

FIGURE 10. Effect of β_e

5. World Health Organization. (2021, November 1). Coronavirus disease (COVID-19): How is it transmitted? World Health Organization. https://www.who.int/news-room/q-a-detail/coronavirus-disease-covid-19-how-is-it-transmitted.
6. W. O. Kermack, and A. G. McKendrick. "Contributions to the mathematical theory of epidemics. II.—The problem of endemicity." Proceedings of the Royal Society of London. Series A, Containing Papers of a Mathematical and Physical Character Vol. 138(834), (1932), pp. 55-83, https://doi.org/10.1098/rspa.1932.0171.
7. W. O. Kermack, and A. G. McKendrick. "Contributions to the Mathematical Theory of Epidemics. III.—Further Studies of the Problem of Endemicity." Proceedings of the Royal Society of London. Series A, Containing Papers of a Mathematical and Physical Character Vol.141(843), (1933), pp. 94-122.

8. W. O. Kermack, and A. G. McKendrick. "Contributions to the Mathematical Theory of Epidemics—II. The Problem of Endemicity." Bulletin of Mathematical Biology Vol. 53 (1-2), (1991), pp. 57-87, https://doi.org/10.1007/bf02464424.
9. S. Mandal, T. Bhatnagar, N. Arinaminpathy, A. Agarwal, A. Chowdhury, M. Murhekar, S. Sarkar, S. Prudent Public Health Intervention Strategies to Control the Coronavirus Disease 2019 Transmission in India: A Mathematical Model-Based Approach. The Indian Journal of Medical Research, Vol. 151(2-3), (2020) pp. 190-199.
10. M. Naveed, M. Rafiq, A. Raza, N. Ahmed, I. Khan, K.S. Nisar, A. H.Soori, Mathematical Analysis of Novel Coronavirus (2019-nCov) Delay Pandemic Model. Comput. Mater. Continua, Vol. 64(3), (2020). pp. 1401-1414, https://doi.org/10.32604/cmc.2020.011314.
11. O. Oren, S.L. Kopecky, T. J. Gluckman, B. J. Gersh, R.S. Blumenthal, Coronavirus Disease 2019 (COVID-19): Epidemiology, Clinical Spectrum and Implications for the Cardiovascular Clinician. American College of Cardiology (2020).
12. S. Saha, S. Saha, The impact of the undetected COVID-19 cases on its transmission dynamics. Indian Journal of Pure and Applied Mathematics, (2020), pp. 1-6.
13. A.S. Shaikh, I.N. Shaikh, K.S. Nisar, A Mathematical Model of COVID-19 Using Fractional Derivative: Outbreak in India with Dynamics of Transmission and Control. Advances in Difference Equations, Vol.373, (2020), (1), pp. 1-19, https://doi.org/10.1186/s13662-020-02834-3.
14. S. Sharma and P.K. Sharma, Stability Analysis of an SIR Model with Alert Class Modified Saturated Incidence Rate and Holling Functional Type-II Treatment, DE GRUYTER Computational and Mathematical Biophysics ISSN: 2544-7297, 2023, Vol-11, Issue-1,Page: 1-10.https://doi.org/10.1515/cmb-2022-0145.
15. S. Umdekar , P.K. Sharma, and S. Sharma, An SEIR model with modified saturated incidence rate and Holling type II treatment function, DE GRUYTER Computational and Mathematical Biophysics ISSN: 2544-7297, 2023, Vol-11, Issue-1, Page: 1-14.https://doi.org/10.1515/cmb-2022-0146.
16. S. Sharma, and P.K. Sharma, A study of SIQR model with Holling type–II incidence rate, Malaya Journal of Matematik, ISSN(O):2321-5666, Vol. 9, No. 1, 305-311, https://doi.org/10.26637/MJM0901/0052.
17. Soni, M., Sharma, R. K., & Sharma, S. (2021). The basic reproduction number and herd immunity for COVID-19 in India. Indian Journal of Science and Technology, 14(35), 2773-2777, https ://doi.org/10.17485/IJST/v14i35.797.
18. Soni, M., Sharma, R. K., & Sharma, S. (2024). PREVENTION STRATEGIES TO CONTROL AN EPIDEMIC USING A SEIQHRV MODEL. The Pure and Applied Mathematics, 31(2), 131-158, https://doi.org/10.7468/jksmeb.2024.31.2.131.
19. P. Van den Driessche, Reproduction numbers of infectious disease models. Infectious Disease Modelling, Vol. 2(3), (2017), pp. 288-303, https://doi.org/10.1016/j.idm.2017.06.002.
20. C. Yang, J. Wang, A Mathematical Model for the Novel Coronavirus Epidemic in Wuhan, China. Mathematical Biosciences and Engineering: MBE, Vol. 17(3) (2020), 2708. https://doi.org/10.3934/mbe.2020148.